ELSEVIER

Journal of Photochemistry and Photobiology A: Chemistry 112 (1998) 103–109

Journal of Photochemistry and Photobiology A:Chemistry

# Application of the transient grating technique to the study of the energetics and dynamics of electron transfer reactions: separation of an ion pair into free ions [1]

Eric Vauthey *, Arthur Henseler

*Institute of Physical Chemistry of the University of Fribourg, Pérolles, CH-1700 Fribourg, Switzerland*

## Abstract

The enthalpy of formation of the free ions generated by the electron transfer between benzophenone in the lower triplet state and 1,4-diazabicyclo[2,2,2]octane in acetonitrile has been measured using transient thermal phase grating. This enthalpy is smaller by more than $0.14 \pm 0.08$ eV than the enthalpy of formation of the geminate ion pair obtained from a previous ps thermal phase grating investigation. Therefore, the dissociation of a geminate ion pair into free ions in endothermic. However, separation is exergonic if translational entropy in taken into account. A small and positive value of *C*, the correction term in the Rehm–Weller equation, is obtained if this term is considered as a free energy. The principles of the transient grating technique as a tool for investigating photoinduced processes in solution are briefly reviewed. © 1998 Elsevier Science S.A.

*Keywords:* Free ions; Enthalpy; Transient grating technique

## 1. Introduction

Although the general scheme for intermolecular photoinduced electron transfer (ET) reaction is now well accepted [1], the energetics of this process is still controversial. The free energy change for the reaction: encounter complex → ion pair, $\Delta G_{ET}$, is usually calculated from the Rehm–Weller equation [2]:

$$\Delta G_{ET} = E_{ox}(D) - E_{red}(A) - E^* + C \quad (1)$$

where $E_{ox}(D)$ and $E_{red}(A)$ are the oxidation and reduction potentials of the donor and acceptor respectively, $E^*$ the energy of the excited state and $C$ a correction term, also called Coulomb term, taking into account the energy gained by bringing the two radical ions at ET distance [2]. Several expressions have been proposed for this term, predicting either negligible or substantial electrostatic interactions in polar solvents [2–4].

Experimentally, $\Delta H_{ET}$ can be determined by using time-resolved photothermal spectroscopy. The most widely applied techniques are the thermal lensing and the photoacoustic spectroscopies [5]. However, the time response of these two methods is too low to resolve heat deposition processes taking place in the sub-ns timescale as it is the case with ET quenching. The transient grating technique offers the highest time resolution to study heat releasing processes [6]. The use of this technique is still scarce in chemistry, but it has already proven to be a powerful method to study various processes, such as protein motion [7] and the dynamics and thermodynamics of excited states [8–10], taking place in a timescale ranging from a few ps to a few μs.

Recently, we reported on a study of the ET between benzophenone (BP) in the triplet state and 1,4-diazabicyclo[2,2,2]octane (DABCO) in acetonitrile (MeCN) using the ps transient grating technique [11]. This investigation allowed the enthalpy of ET from $^3BP^*$ to be determined. Considering the time scale of the experiment, this enthalpy corresponds essentially to the enthalpy of formation of the ion pair, $\Delta H_{ip}$ (see Fig. 1). The magnitude of the Coulomb term was estimated to be of the order of $-0.28$ eV by comparing the experimental $\Delta H_{ip}$ to $\Delta G_{ET}$ calculated from the Rehm–Weller equation. However, such a comparison requires the knowledge of the entropy difference upon ET, $\Delta S_{ET}$, and of the exact redox potentials of the reaction partners. Therefore, the magnitude of $C$ determined in this way may contain a substantial error originating from the uncer-

---

* Corresponding author. Tel.: +41-26-3008711 (15); fax: +41-26-3009737; e-mail: eric.vauthey@unifr.ch.

[1] The publisher regrets, this paper, which was scheduled for the special issue on the XVII International Conference on Photochemistry, is only published now.

1010-6030/98/$19.00 © 1998 Elsevier Science S.A. All rights reserved
*PII* S1010-6030(97)00283-9

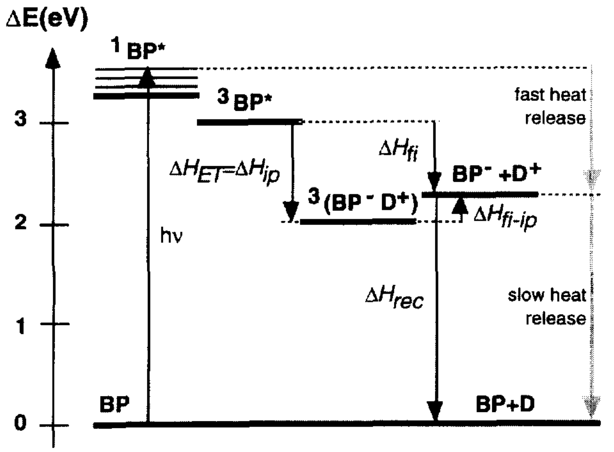

Fig. 1. Energy diagram of the states involved in the photoinduced ET between BP and DABCO in MeCN (D = DABCO) (the separation between fast and slow heat releases pertains to the TTPG experiment with cw detection).

tainty in $\Delta S_{\mathrm{ET}}$, $E_{\mathrm{ox}}(\mathrm{D})$ and $E_{\mathrm{red}}(\mathrm{A})$. Moreover, $C$ was assumed to be a potential energy. However, as it will be discussed below, $C$ should actually be considered as a free energy.

In this paper, we first present the principles of the transient grating technique and show its possibilities and limitations. We then report on the measurement of the enthalpy of formation of the free ions, $\Delta H_{\mathrm{fi}}$, in the ET between $^3\mathrm{BP}^*$ and DABCO in MeCN using the transient thermal phase grating technique with cw detection. In order to eliminate the uncertainties arising from the comparison of $\Delta H_{\mathrm{ip}}$ with $\Delta G_{\mathrm{ET}}$, the magnitude of $C$ is estimated by comparing $\Delta H_{\mathrm{ip}}$ with $\Delta H_{\mathrm{fi}}$ (see Fig. 1).

## 2. Principles of the transient grating technique

In a transient grating experiment, the sample is excited by two spatially crossed and time coincident laser pulses producing an interference pattern, as shown in Fig. 2a [12]. This spatially modulated excitation creates in the sample spatial distributions of ground state, excited state and/or photochemical intermediate and product populations. Consequently, similar modulations of the refractive index and absorbance are generated.

The modulation amplitude of the absorbance, $\Delta A$, depends directly on the concentration changes, $\Delta C$ of each component $i$ with an extinction coefficient $\varepsilon$:

$$\Delta A(\lambda,t)=\sum_i \varepsilon_1(\lambda)\Delta C_i(t) \tag{2}$$

The modulation amplitude of the refractive index, $\Delta n$, contains two contributions: one which depends on the population changes, $\Delta n_{\mathrm{pop}}$, and one which depends on the change of density, $\Delta n_{\mathrm{d}}$:

$$\Delta n=\Delta n_{\mathrm{pop}}+\Delta n_{\mathrm{d}} \tag{3}$$

$$\Delta n_{\mathrm{pop}}(\lambda,t)=\frac{(n^2+2)^2}{6n}\sum_i R_i(\lambda)\Delta C_i(t) \tag{4}$$

$$\Delta n_{\mathrm{d}}(t)=\sum_{ji} c\left(\frac{aQ_j}{\rho C_\nu}+\Delta V_j\right)\rho\frac{\partial n}{\partial\rho}f(k_{\mathrm{r},j},t) \tag{5}$$

where $n$ is the average refractive index, $R_i$ the molar refractivity of component $i$, $c$ a constant, $a$ the coefficient of thermal expansion of the solvent, $\rho$ its density, $C_\nu$ its heat capacity, $Q_j$ the amount of heat released during process $j$ and $\Delta V_j$ the change of volume during the same process. Finally, $f(k_{\mathrm{r},j},k_{\mathrm{td}},t)$ is a function which depends on the rate constant, $k_{\mathrm{r}}$, of the heat releasing process $j$, on the geometry of the experiment, and on various acoustic properties of the sample [8]. Eq. (5) is only valid in the limit where the decay of the density phase grating by both thermal diffusion and translational diffusion is negligible.

The amplitude of these grating-like distributions can be measured by a third, time-delayed laser pulse, or a cw laser beam, striking the grating at Bragg angle (see Fig. 2b). The relationship between the diffracted intensity and the amplitude of the modulations at the probing wavelength can be calculated with the following equation proposed by Kogelnik for a plane-wave hologram [13]:

$$\eta=\frac{I_{\mathrm{dif}}}{I_{\mathrm{inc}}}\approx\left[\left(\frac{\pi(\Delta n_{\mathrm{pop}}+\Delta n_{\mathrm{d}})d}{\lambda\cos\theta_{\mathrm{B}}}\right)^2+\left(\frac{1.15\Delta Ad}{2\cos\theta_{\mathrm{B}}}\right)^2\right]\times\exp\left(-\frac{2.3Ad}{\cos\theta_{\mathrm{B}}}\right) \tag{6}$$

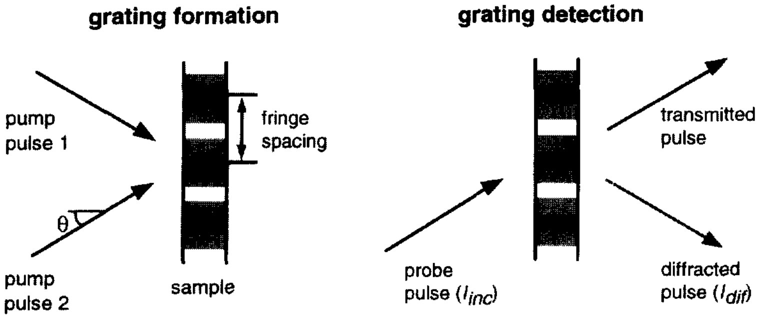

Fig. 2. Schematic illustration of the principle of the transient grating technique.

where $\eta$ is the diffraction efficiency, $I_{\mathrm{dif}}$ and $I_{\mathrm{inc}}$ the diffracted and incident light intensities, $d$ the optical path length, $\theta_B$ the Bragg angle and $A$ the average absorbance of the sample at the probing wavelength, $\lambda$. This equation holds only for diffraction efficiencies smaller than $10^{-2}$ as it is normally the case in the transient grating technique. In order to have a better understanding of this equation, several special cases can be considered.

### 2.1. Pure thermal phase gratings: $\Delta A = \Delta n_{pop} = 0$ at $\lambda$; $\eta \propto \Delta n_d^2$

In this case, the only contribution to the diffraction efficiency is due the refractive index grating (phase grating) induced by the modulation of the density. As in most organic solvents $\Delta n_d$ is due to a large extent to the first term in brackets of Eq. (5), i.e., thermal induced change of density, this type of grating is called *thermal phase grating*. An important parameter governing the time evolution of the diffracted intensity is the acoustic period $\tau_{ac}$, which corresponds to the time needed for the material in an illuminated fringe of the grating to adopt its new density [14]:

$$\tau_{ac} = \frac{\Lambda}{\nu_s} = \frac{\lambda_e}{2 \sin \theta_e \nu_s} \qquad (7)$$

where $\Lambda$ is the fringe spacing, $\nu_s$ the speed of sound, $\lambda_e$ the excitation wavelength and $\theta_e$, the angle of incidence of the excitation pulses. When heat is released within a time shorter than $\tau_{ac}$, the thermal grating signal is completely modulated by the acoustic response: two counterpropagating waves are generated and the density at the grating peaks oscillates between normal and a reduced value while the density at grating nulls oscillates between normal and an increased value (see Fig. 3a). On the other hand, when $k_r^{-1} > \tau_{ac}$, the acoustic response is no longer driven impulsively and the dynamics of the heat deposition can be resolved, as shown in Fig. 3b.

### 2.2. Pure population gratings: $\Delta n_d = 0$ or $\theta_e \approx 0$; $\eta \propto \Delta n_{pop}^2 + \Delta A^2$

If no density change occur, the diffraction efficiency depends only on the amplitude ($\Delta A$) and phase ($\Delta n_{\mathrm{pop}}$) population gratings. Consequently, the diffracted intensity is directly proportional to the square of the concentration changes. In this case, the transient grating technique can be an alternative to transient absorption spectroscopy [15,16]. If $\Delta n_d \neq 0$, the pure population grating can still be detected by increasing the acoustic period. By exciting at 355 nm with $\theta_e = 0.2°$, the acoustic period becomes as large as 40 ns in acetonitrile (MeCN). During the first few ns after excitation, the diffracted intensity contents only contributions from population gratings and is not 'contaminated' by the thermal phase grating. For example, Fig. 4 shows the time evolution of the diffracted intensity measured at 630 nm after excitation at 355 nm of a solution of 9,10-dicyanoanthracene (DCA) with 0.1 M naphthalene (NAP) in MeCN with $\theta_e = 0.2°$. This signal corresponds essentially to the decay of the $S_n \leftarrow S_1$ absorption of DCA upon diffusional ET quenching by NAP.

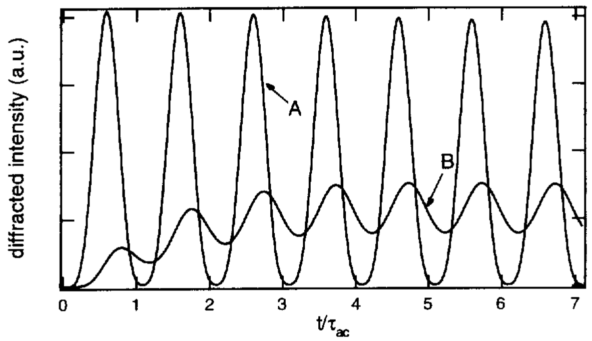

Fig. 3. Calculated time profiles of the diffracted intensity due to pure thermal phase grating for two different rate constants of heat deposition, $k_r$: (A) $k_r = 10\,\tau_{ac}^{-1}$; (B) $k_r = \tau_{ac}^{-1}$.

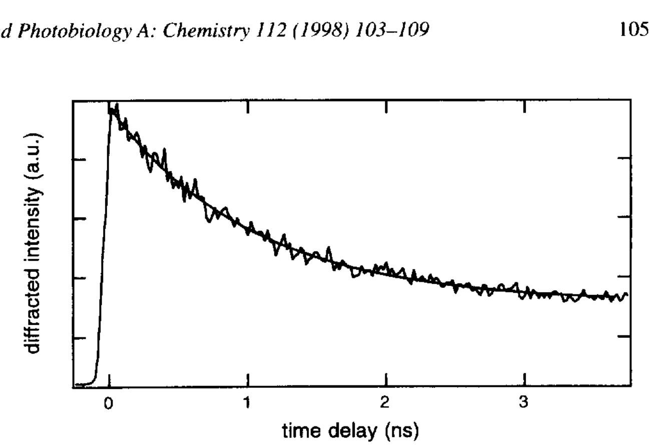

Fig. 4. Time profile of the diffracted intensity measured at 630 nm after exciting at 355 nm a solution of DCA and 0.1 M NAP in MeCN with an angle of incidence of 0.2°.

The contribution of the thermal phase grating can also be eliminated by exciting the sample with perpendicularly polarised pump pulses. In this case, there is no spatial distribution of pump intensity, hence no modulation of density [17,18]. However, the polarisation of the pump light on the sample is spatially modulated. The time evolution of the diffracted intensity from such a polarisation grating reflects the time dependence of the polarisation anisotropy related to the population monitored at the probe wavelength.

### 2.3. Mixed gratings: $\Delta A$, $\Delta n_{pop}$ and $\Delta n_d \neq 0$ at $\lambda$; $\eta \propto (\Delta n_{pop} + \Delta n_d)^2 + \Delta A^2$

The contributions of the population phase grating and of the thermal phase grating to the diffraction efficiency interfere through the cross term $2\Delta n_{\mathrm{pop}}\Delta n_{\mathrm{d}}$. This interference is especially important when the amplitudes of both gratings are of the same order of magnitude and its nature depends on the sign of the refractive index changes [11,19]. The thermoinduced change of refractive index is always negative, while the change of refractive index related to the population can be of either sign. Fig. 5 shows the calculated time profile of the diffracted intensity for a mixed population and thermal phase grating with positive and negative $\Delta n_d / \Delta n_{\mathrm{pop}}$ ratios. In Fig. 5a, $\Delta n_{\mathrm{pop}}$ and $\Delta n_d$ have the same sign, the interference

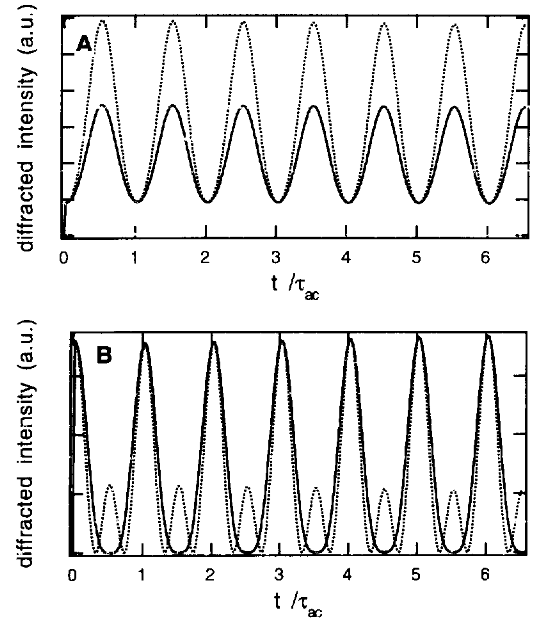

Fig. 5. Calculated time profiles of the diffracted intensity illustrating the interference between population and thermal phase gratings. (A) Constructive interference: $R = \Delta n_d/\Delta n_{pop} = 1$ (solid line); $R = 1.5$ (dotted line). (B) Destructive interference: $R = -1$ (solid line); $R = -1.5$ (dotted line).

is constructive. In Fig. 5b, $\Delta n_{pop}$ and $\Delta n_d$ have opposite signs and the interference is destructive. When $|\Delta n_d| = |\Delta n_{pop}|$, the population phase grating is completely modulated by the thermal phase grating and the intensity maxima are out phase with those occurring with positive interference. When $|\Delta n_d| > |\Delta n_{pop}|$, diffracted intensity maxima in phase with those of Fig. 5a begin to emerge between the initial peaks. As $|\Delta n_t|$ increases further, these new diffracted intensity maxima dominate and the time profile becomes very similar to the case of constructive interference. The analysis of the time profile of diffracted intensity in the case of mixed grating can be rather complex. Fig. 6 shows the time profile of the diffracted intensity at 532 nm after excitation at 355 nm with $\theta_e = 25°$ of a solution of 9-cyanophenanthrene (CNP) with various amounts of *N*,*N*-dimethylaniline (DMA) in MeCN. Without DMA, the diffraction is due to the population grating of $^1$CNP* interfering constructively with the thermal phase grating induced by the release as heat of the excitation excess energy. The decrease of the oscillation is due to acoustic attenuation and to the decay of the population, hence of the constructive interference. With 1 M DMA, a double oscillation caused by a destructive interference can be observed. In this case, the oscillation originates from the heat released upon ET quenching of $^1$CNP* by DMA, interfering destructively with the population gratings of DMA$\cdot^+$ and CNP$\cdot^-$, which both have a positive molar refractivity at 532 nm. At intermediate concentrations, the effects seen with [DMA] = 0 and [DMA] = 1 M counterbalance, and the time profile exhibits almost no oscillation.

The above discussion shows that many processes can contribute to a transient grating signal. Therefore, the system to be studied and the experimental condition must be carefully chosen.

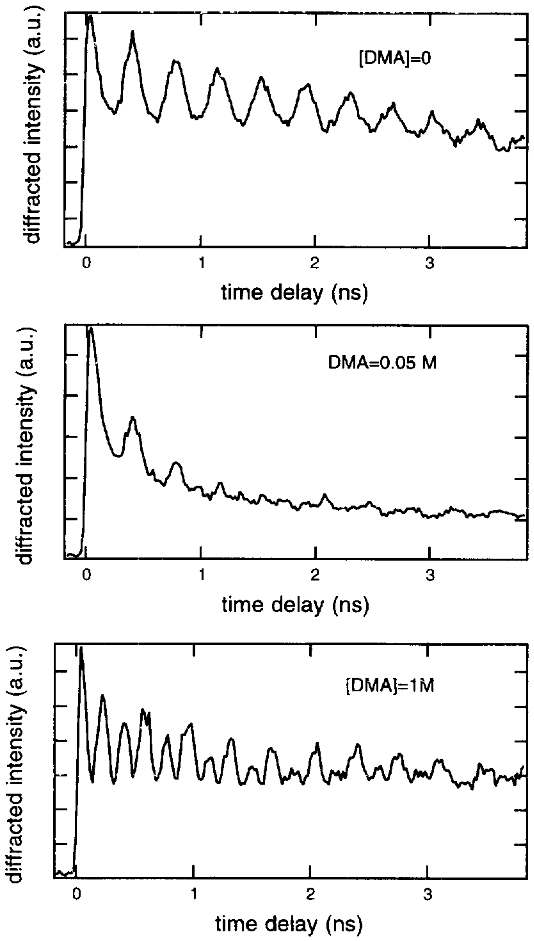

Fig. 6. Time profiles of the diffracted intensity measured at 532 nm after exciting at 355 nm a solution of CNP with various concentration of DMA in MeCN with an angle of incidence of 25°.

## 3. Experimental

### 3.1. Apparatus

The transient grating set up has been described in details in Ref. [11] (pump-probe detection) and in Ref. [20] (NIR cw-detection).

### 3.2. Samples

Benzophenone, BP (Aldrich), was twice recristallised from aqueous ethanol and sublimed under vacuum. 1,4-Diazabicyclooctane, DABCO (Fluka), was recristallised from a 1:1 benzene–hexane mixture and then twice sublimed under vacuum. Acetonitrile, MeCN (Fluka), was of spectroscopic grade and was used as such. During sample preparation, a great care was taken to avoid contamination by water. The concentration of BP was about 10 mM corresponding to an

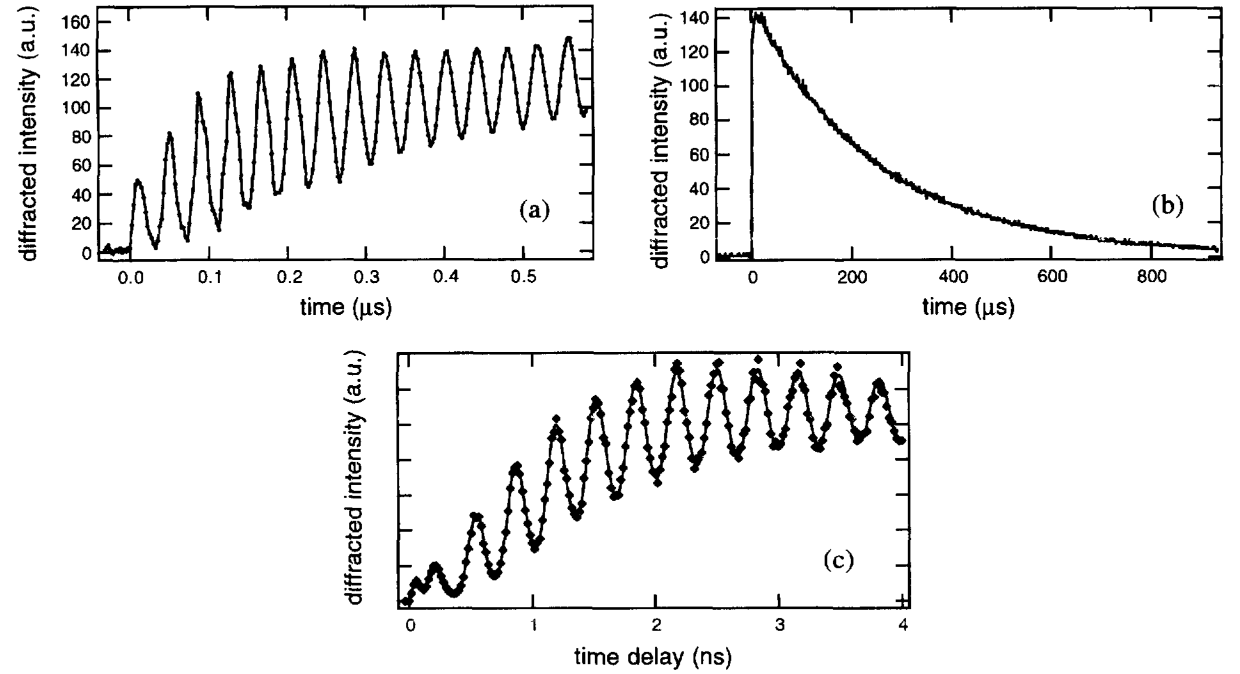

Fig. 7. (A,B) Time profiles at different time scales of the diffracted intensity measured at 1064 nm after excitation at 355 nm of a solution of BP with 0.1 M DABCO in MeCN. (C) Time profile of the diffracted intensity measured at 590 nm with the ps setup using an angle of incidence of 22° with the same solution as above and best fit of Eq. (3) of Ref. [11] with acoustic attenuation (solid line).

absorbance at 355 nm of 0.2 on 1 mm, the cell thickness. All measurements were carried out at 20 ± 0.5°C.

## 4. Results and discussion

The time profile of the diffracted intensity at 1064 nm after excitation at 355 nm of a solution of BP and 0.10 M DABCO in MeCN is shown in Fig. 7a,b. The initial oscillation is due to heat released in a time shorter than the acoustic time of the sample, $\tau_{ac}$. At 355 nm and with an angle of incidence of about 0.27°, the acoustic time amounts to 31 ns in MeCN. Therefore, this oscillation is caused by the heat released during the various transitions from the vibrationally unrelaxed singlet excited state of BP to the free ions, the slower step being the separation of the geminate ion pair to free ions with a rate constant of the order of $2\text{–}5 \times 10^{8}\ s^{-1}$ as shown in Fig. 1. The slow rising dc component corresponds to heat released with a time constant larger than $\tau_{ac}$, i.e., the heat due to homogeneous recombination of the free ions to the neutral ground state. The decay of the diffracted signal shown in Fig. 7b is due to thermal diffusion. Subtracting the enthalpy of free ion recombination, $\Delta H_{rec}$, from the energy of $^{3}BP^{*}$ ($E^{*} = 3.0$ eV) gives the enthalpy of formation of the free ions, $\Delta H_{fi}$. The enthalpy of free ion recombination is itself obtained by comparing the amplitudes of the slow to fast heat releases as described in Refs. [20,21]. The applicability of this procedure to recover the energetics of a process following second order kinetics is discussed in Ref. [21]. Its main advantage is that it does not require any fit as long as there is no interference with population gratings. The presence of a population grating due to $BP^{\cdot -}$ at 1064 nm has been determined by measuring the diffraction efficiency in the 0–4 ns time window using the ps setup. Its contribution is almost undetectable and is completely negligible in view of the very large amount of heat released. If it were not the case, a double oscillation which is typical of a destructive interference between population and thermal phase gratings as expected at this wavelength would be observe. The measurements were carried out with 0.05, 0.1 and 0.2 M DABCO and exhibit the same slow to fast heat ratio, resulting in $\Delta H_{fi} = -0.76 \pm 0.04$ eV. This value is in excellent agreement with that measured by photoacoustic spectroscopy by Goodman and Peters ($\Delta H_{fi} = -0.74$ eV) [22]. These two enthalpies have been obtained by assuming no volume change and a free ion yield of unity as reported by Haselbach et al. [23]. A smaller ion yield of 0.8 has been reported by Miyasaka et al. [24]. However, this value was measured at high DABCO concentrations, where quenching of $^{1}BP^{*}$ can take place. The back ET within the resulting singlet geminate ion pair is faster than separation, and therefore the ion yield decreases [25]. If an ion yield smaller than unity were assumed, $\Delta H_{fi}$ would be even less negative.

In the ps experiment reported in detail in [11], the angle of incidence was 15°, $\tau_{ac}$ equal to 560 ps and the time window of the experiment between 0 and 4 ns. Fast heat was due to the formation of $^{3}BP^{*}$ and slow heat to ET generating the geminate ion pair. No heat releasing or absorbing process due to the formation of the free ions from the geminate ion pair was observed within the time window of the experiment. New ps measurements with a larger angle of incidence ($\tau_{ac} = 330$ ps) and DABCO concentrations of 0.1 and 0.2 M were carried out to obtain a better signal to noise ratio (see Fig. 7c). These data confirmed the previously obtained value of $\Delta H_{ip} = -0.94 \pm 0.04$ eV, assuming no volume change.

Comparison of these two values shows that the enthalpy of formation of the free ions is less negative by $0.18 \pm 0.08$ eV than the enthalpy of formation of geminate ion pair, i.e., that the enthalpy of separation of the ion pair, $\Delta H_{fi-ip}$, amounts to $0.18 \pm 0.08$ eV. This difference cannot be ascribed to the assumption of a free ion yield equal to unity as discussed above. Transient thermal phase grating spectroscopy detects variations of refractive index induced by changes of density. Electrostriction as well as changes of molecular volume also contribute to the change of density (see Eq. (5)). The change of volume, $\Delta V$, upon separation of a geminate radical ion pair into free ions in MeCN is not known. By comparison with volume changes measured for the dissociation of inorganic salts and organic charge transfer complexes, $\Delta V$ can be expected to lie between 0 and $-5$ ml mol$^{-1}$ for the separation of a geminate ion pair [26]. The volume change, if any, related to the separation of the ions (without considering the solvent), $\Delta V_{ion}$, can be expected to be slightly positive. However, it could be compensated by a negative volume change due to larger electrostriction of the solvent around the free ions. This volume change caused by electrostriction, $\Delta V_{solv}$, can be calculated from the pressure derivative of the difference of solvation energy between free ions and ion pair: $\Delta V_{solv} = \partial \Delta G_{solv} / \partial P$ [27]. The magnitude of $\Delta G_{solv}$ is not known experimentally and is a matter of controversy as discussed below. Assuming $\Delta V_{ion} = 0$ and $\Delta V_{solv} = -5$ ml mol$^{-1}$, the enthalpy of formation of free ion is still less negative by 0.12 eV than the enthalpy of formation of the geminate ion pair.

This enthalpy difference reveals that the separation of the geminate ion pair is endothermic. It is however well know, that in polar solvents, the separation of the ion pair occurs very efficiently. Therefore, the equilibrium between ion pair and free ions can be expected to be strongly in favour of free ions, indicating that separation must be exergonic. If this is the case, this process must be entropy driven. The entropy change associate to ionic dissociation, $\Delta S_{fi-ip}$, comprises a contribution associated to solvation given by $\Delta S_{solv} = -\partial \Delta G_{solv} / \partial T$, which could be slightly negative upon separation (vide infra) and a contribution of translational entropy of the ions, $\Delta S_{tr}$. The latter has been estimated to be as large as $10^{-3}$ eV K$^{-1}$ for an ion concentration of $10^{-6}$ M, resulting in an energy $T\Delta S_{tr}$ of 0.3 eV at room temperature [28]. Moreover, Knibbe et al. have determined a $T\Delta S$ value of $-0.23$ eV for exciplex formation in non polar solvents [29]. The formation and dissociation of the encounter complex are due to random motion of the reactants. Thus its free energy is the same as that of the free reactants and the term $C$ in Eq. (1) is equal to (see Fig. 8):

$$C = \Delta G_{ip} - \Delta G_{fi} = -\Delta G_{fi-ip} = -(\Delta H_{fi-ip} - T\Delta S_{fi-ip}) \qquad (8)$$

A more precise estimation of the electrostatic interaction within the ion pair and of $C$ from the measured $\Delta H_{fi-ip}$ requires the knowledge of the change of solvation energy upon separation, $\Delta G_{solv}$, in order to estimate both $\Delta V_{solv}$ and $\Delta S_{solv}$. Two models resulting to substantially different magnitudes of $\Delta G_{solv}$ have to be considered.

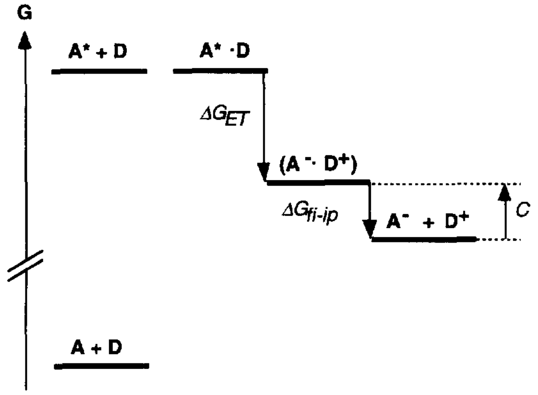

Fig. 8. Free energy diagram of the states involved in an intermolecular photoinduced ET reaction in polar solvents.

### 4.1. $\Delta G_{solv} \approx 0$

If one assumes that the solvation energy of the free ions is the same as that of the geminate ion pair, then $C$ is equal to $-(\Delta H_{fi-ip} - T\Delta S_{tr})$ and $\Delta H_{fi-ip}$, originates from electrostatic interaction between the ions. Using the Onsager model for the solvation energy of a dipole and the Born equation for the solvation energy of ions, Suppan showed that the solvation energies of geminate ion pair and free ions in a polar solvent are almost identical [28]. Therefore, $\Delta S_{solv} = \Delta V_{solv} = 0$ and the electrostatic interaction within the geminate ion pair is of the order of $-0.18 \pm 0.08$ eV, which is less negative than that deduced from the ps experiment alone with the various sources of error mentioned in the introduction. From Eq. (8) with 0.23 eV for $T\Delta S_{tr}$, the correction term $C$ amounts to $+0.05$ eV.

### 4.2. $\Delta G_{solv} \ll 0$

Recently, Tachiya presented a theoretical study of the free energy of formation of ions in solution as a function of their separation distance [4]. According to this work, $\Delta G_{solv}$ is very substantial in polar solvents, contrarily to the prediction of the model used by Suppan. For ions of radius $r$ and assuming contact in the ion pair, $\Delta G_{solv}$ is given by:

$$\Delta G_{solv} = \frac{e^2}{1.9r}\left(1 - \frac{1}{\varepsilon_s}\right) \qquad (9)$$

where $\varepsilon_s$ is the static dielectric constant of the solvent. This expression predicts that the difference of solvation energy between free ions and geminate ion pair is even larger than the solvation energy of one single ion. From Eq. (9), the change of volume due to electrostriction, $\Delta V_{solv}$ is given by:

$$\Delta V_{solv} = \frac{\partial \Delta G_{solv}}{\partial P} = \frac{e^2}{1.9r}\frac{\partial \varepsilon_s^{-1}}{\partial P} \qquad (10)$$

Using $\partial\varepsilon_s^{-1}/\partial P = -1.7\cdot10^{-6}$ bar [30] and $r = 3.5$ Å, $\Delta V_{solv}$ amounts to $-3.5$ ml mol$^{-1}$ and $\Delta H_{fi-ip} = 0.14 \pm 0.08$ eV. In this case however, $\Delta H_{fi-ip}$ is not identical to the electrostatic stabilisation energy, but also contains a contribution form the solvation energy.

The entropy term associated to the difference in solvation energy, $\Delta S_{solv}$ is now different from zero:

$$\Delta S_{solv} = -\frac{\partial\Delta G_{solv}}{\partial T} = -\frac{e^2}{1.9r}\frac{\partial\varepsilon_s^{-1}}{\partial T} \tag{11}$$

with $\partial\varepsilon_s^{-1}/\partial T = 9.3\cdot10^{-5}$ [31] for MeCN, $\Delta S_{solv}$ amounts to $-2.10^{-4}$ eV K$^{-1}$ and $T\Delta S_{solv} = -0.06$ eV at 293 K. From Eq. (8) and with 0.23 eV for $T\Delta S_{tr}$, the correction term $C$ is equal to $+0.03$ eV.

According to Tachiya's expression, which does not take the translational entropy into account, $C$ amounts to $+0.06$ eV for two ions with a radius of 3.5 Å and at contact distance [4]. The enthalpy for ion pair dissociation, $\Delta H_{fi-ip}$ recovered from this expression using Eq. (8) amounts to $-0.12$ eV. According to this model, the dissociation of a ion pair into free ions is exothermic, contrarily to our experimental findings.

Independently on the model used for $\Delta G_{solv}$, the resulting value of the correction term $C$ is positive. This sign is not astonishing if one considers that $C \equiv -\Delta G_{fi-ip}$ and that ion pairs dissociate spontaneously into free ions in polar solvents. In this case, entropy wins over electrostatic stabilisation. In non-polar solvents however, free ions are not formed, indicating that $C$ must be negative. Translation entropy is independent on the solvent, but electrostatic interaction decreases with solvent polarity. In non-polar solvents, electrostatic stabilisation must win over entropy.

The value ascribed to $C$ in our previous paper actually corresponds to $-\Delta H_{fi-ip}$ [11]. In this paper, $C$ was treated as a potential energy but not as a free energy. The original expression of Rehm and Weller for $C$ as well as that of Suppan somehow imply that $C$ is a potential energy. However, if one consider Eq. (1) and Fig. 8, it appears that $C$ is the free energy gained by bringing two ions from 'infinite' distance to ET distance.

## 5. Conclusions

The transient grating technique is very well suited to study the dynamics and the energetics of ET processes. However, we have shown that various processes can contribute to a transient grating signal and therefore the experimental conditions have to be chosen carefully.

Concerning geminate ion pair separation, it is not clear at the present stage whether the enthalpy difference between the free ions state and the geminate ion pair state, $\Delta H_{fi-ip}$, is due to the electrostatic interaction only (i.e., $\Delta G_{solv} \approx 0$) or to electrostatic energy plus a difference of solvation energy between these two states. The validity of the continuum model to calculate the solvation energy of ions in contact and at short distances is questionable. A theoretical treatment of ionic dissociation with a molecular description of the solvent and taking into account the changes in translational entropy is needed.

## Acknowledgements

We wish to thank Professor P. Suppan for helpful discussions. We also express our thanks to Professor E. Haselbach for his continuing support and encouragement. This work was supported by the Fonds National Suisse de la Recherche Scientifique through project number 20-49235.96 and by the Programme d'Encouragement à la Relève Universitaire de la Confédération. Financial support form the Fonds de la Recherche and the Conseil de l'Université de Fribourg is also acknowledged.

## References

[1] M.A. Fox, M. Chanon, Photoinduced Electron Transfer, Elsevier, Amsterdam, 1988.
[2] D. Rehm, A. Weller, Isr. J. Chem. 8 (1970) 259.
[3] P. Suppan, J. Chem. Soc. Far. Trans. I 82 (1986) 509.
[4] M. Tachiya, Chem. Phys. Lett. 230 (1994) 491.
[5] S.E. Braslavsky, G.E. Heibel, Chem. Rev. 92 (1992) 1381.
[6] K.A. Nelson, M.D. Fayer, J. Chem. Phys. 79 (1982) 5202.
[7] L. Richard, L. Genberg, J. Deak, H.L. Chiu, R.J.D. Miller, Biochemistry 31 (1992) 10703.
[8] J. Morais, J. Ma, M. Zimmt, J. Phys. Chem. 95 (1991) 3885.
[9] M. Terazima, N. Hirota, J. Chem. Phys. 95 (1991) 6490.
[10] E. Vauthey, A. Henseler, J. Phys. Chem. 100 (1996) 170.
[11] E. Vauthey, A. Henseler, J. Phys. Chem. 99 (1995) 8652.
[12] H.J. Eichler, P. Günter, D.W. Pohl, Laser-Induced Dynamic Gratings, Springer Verlag, Berlin, 1986.
[13] H. Kogelnik, Bell. Syst. Tech. J. 48 (1969) 2909.
[14] L. Genberg, Q. Bao, S. Gracewski, R.J.D. Miller, Chem. Phys. 131 (1989) 81.
[15] E. Vauthey, Chem. Phys. 196 (1995) 569.
[16] C. Högemann, M. Pauchard, E. Vauthey, Rev. Sci. Instrum. 67 (1996) 3449.
[17] F.W. Deeg, M.D. Fayer, J. Chem. Phys. 91 (1989) 2269.
[18] J.C. Gumy, E. Vauthey, J. Phys. Chem. 100 (1996) 8628.
[19] K.A. Nelson, R. Casalegno, R.J.D. Miller, M.D. Fayer, J. Chem. Phys. 77 (1982) 1144.
[20] A. Henseler, E. Vauthey, J. Photochem. Photobiol. A 91 (1995) 7.
[21] E. Vauthey, J. Photochem. Photobiol. A 109 (1997) 195.
[22] J.L. Goodman, K.S. Peters, J. Am. Chem. Soc. 108 (1986) 1700.
[23] E. Haselbach, E. Vauthey, P. Suppan, Tetrahedron 44 (1988) 7335.
[24] H. Miyasaka, K. Morita, K. Kamada, N. Mataga, Chem. Phys. Lett. 178 (1991) 504.
[25] K.S. Peters, J. Lee, J. Phys. Chem. 97 (1993) 3761.
[26] T. Asano, W.J.L. Noble, Chem. Rev. 78 (1978) 407.
[27] E. Whalley, J. Chem. Phys. 38 (1963) 1400.
[28] P. Suppan, Chimia 42 (1988) 320.
[29] H. Knibbe, D. Rehm, A. Weller, Ber. Bunsenges. Phys. Chem. 73 (1969) 839.
[30] E.U. Franck, Organic Liquids: Structure, Dynamics and Chemical Properties, Wiley, New York, 1978.
[31] G.J. Janz, R.P.T. Tomkins, Nonaqueous Electrolytes Handbook, Academic Press, New York, 1972.